91. Synthesis, Isolation, and Full Spectroscopic Characterization of Eleven (*Z*)-Isomers of (3*R*,3'*R*)-Zeaxanthin

by **Gerhard Englert, Klaus Noack, Emil A. Broger, Ernst Glinz, Max Vecchi**[1]), and **Reinhard Zell***

Pharma Research & Development, *F. Hoffmann-La Roche AG*, CH–4002 Basel

(6.V.91)

Developmental efforts to improve the yield of the chemical synthesis of (3*R*,3'*R*)-zeaxanthin resulted in the isolation, partly by chromatography from reaction mixtures, and full spectroscopic characterization by ^{1}H-NMR, UV/VIS, and CD spectrosocpy of eleven (*Z*/*E*)-isomers of zeaxanthin: (7*Z*)-, (9*Z*)-, (13*Z*)-, (15*Z*)-, (7*Z*,7'*Z*)-, (9*Z*,9'*Z*)- (7*Z*,9*Z*,7'*Z*)-, (7*Z*,11*Z*,7'*Z*)-, (9*Z*,13*Z*,9'*Z*)-, (7*Z*,9*Z*,7'*Z*,9'*Z*)-, and (7*Z*,9*Z*,11*Z*,7'*Z*,9'*Z*)-zeaxanthin. Five of these isomers were obtained by specific synthesis, namely the (7*Z*)-, (7*Z*,7'*Z*)-, (9*Z*,9'*Z*)-, (7*Z*,9*Z*,7'*Z*)-, and (7*Z*,9*Z*,7'*Z*,9'*Z*)-isomers.

1. Introduction. – Starting from the optically pure hydroxyketone **1**, an efficient synthesis of (3*R*,3'*R*)-zeaxanthin (**2**) was described recently [1]. The final step involves a double *Wittig* condensation. Developmental efforts to improve the yield of **2** have

Scheme. *Synthesis of* (Z,E)*-Zeaxanthenals and* (Z,E)*-Zeaxanthins*

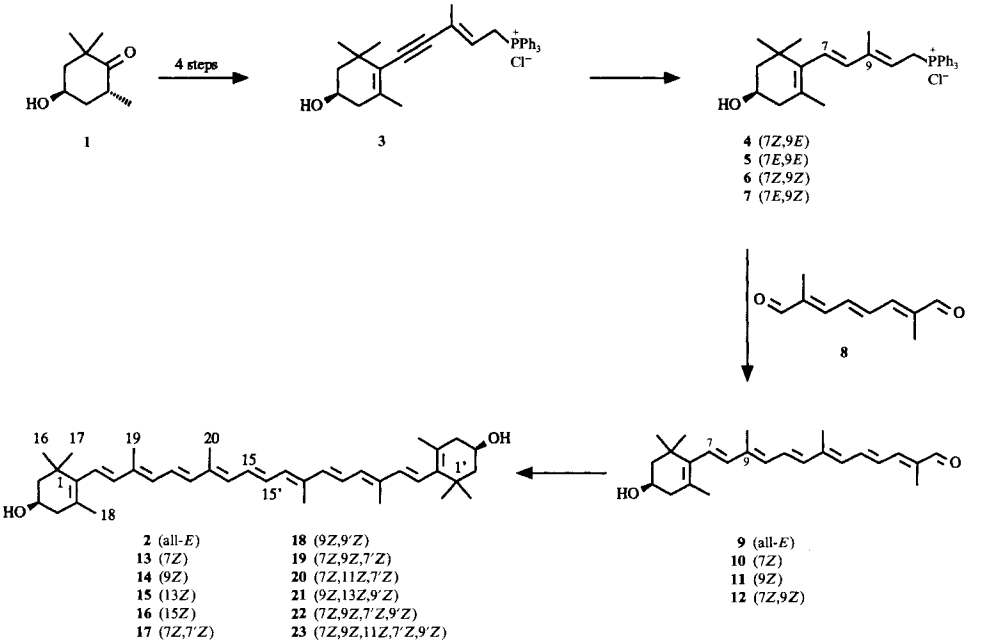

[1]) Deceased 1989.

resulted in the isolation and full spectroscopic characterization of eleven (*Z*/*E*)-isomers of zeaxanthin. In addition, five of these isomers were also prepared by specific synthesis (see *Scheme* and *Table 1*). We wish to report on the details of this work.

2. Synthesis of (*E*/*Z*)-Isomers. – From hydroxyketone **1**, the acetylenic phosphonium salt **3** [1] was prepared. Partial hydrogenation of (9*E*)-**3** [2] with *Raney*-Ni and Pd^{II}-catalyzed isomerization resulted in the formation of the olefinic phosphonium salts **4** ((7*Z*,9*E*)) [1] and **5** ((7*E*,9*E*); [1]; see also [3–8]). On the other hand, use of (9*Z*)-**3** led to the new isomers **6** ((7*Z*,9*Z*)) and **7** ((7*E*,9*Z*)) without problems. However, the hydrogenation of the (9*Z*)-isomer proceeded considerably slower than that of the (9*E*)-isomer.

Having these new (9*Z*)-phosphonium salts at hand, it appeared attractive to synthesize specifically some of the (*Z*)-isomeric zeaxanthins now accessible. Mono *Wittig* condensation of the respective phosphonium salt with the C_{10}-dialdehyde **8** [9] to form the C_{25}-apocarotenals was carried out in refluxing EtOH with 1,2-epoxybutane as acid scavenger. The latter has been successfully used for this purpose already as early as 1968 [10]. Since formation of minor amounts of C_{40}-polyenes due to double *Wittig* condensation could not be avoided, the products had to be further purified by flash chromatography. In this way, the following isomers of **9** were synthesized and for the first time fully characterized (*Table 1*): **10** ((7*Z*); yield 51.8%; HPLC 96.2%), **11** ((9*Z*); yield 31.8%, HPLC 99.9%), and **12** ((7*Z*,9*Z*); yield 16.5%, HPLC 98.0%). Previously, only the (9*Z*)-isomer **11** was known. It had been prepared by *Szabolcs* and coworkers through oxidative degradation of neolutein B ([11]; λ_{max} 404 nm (hexane)) and of antheraxanthin diacetate [12]. Structure analysis was based on UV/VIS data, mixed chromatograms, reversible tests, *etc.* The (all-*E*)-C_{25}-hydroxy-apocarotenal **9** had previously been prepared and fully characterized by different groups [13] [14] [6].

So far, only a limited number of (*Z*)-zeaxanthins is known from the literature. Isomers **14** ((9*Z*); neozeaxanthin B) and **15** ((13*Z*); neozeaxanthin A) were obtained by I_2-catalyzed stereomutation of the (all-*E*)-isomer **2** [11] [15–17]. ^{13}C-NMR data are specified in [11], CD data in [17]. In addition, **16** ((15*Z*)) and **18** ((9*Z*,9′*Z*)) were isolated from synthetic mixtures [18] [19] and their CD and UV data determined [20]. Isomers **15**

Table 1. *Isomeric Zeaxanthinals* **9–12** *and Zeaxanthins* **13–23**

	Configuration	Synthetic	Isolated by HPLC
9	(7*E*,9*E*)	+	
10	(7*Z*)	+	
11	(9*Z*)	+	
12	(7*Z*,9*Z*)	+	
13	(7*Z*)	+	+
14	(9*Z*)		+
15	(13*Z*)		+
16	(15*Z*)		+
17	(7*Z*,7′*Z*)	+	+
18	(9*Z*,9′*Z*)	+	+
19	(7*Z*,9*Z*,7′*Z*)	+	+
20	(7*Z*,11*Z*,7′*Z*)		+
21	(9*Z*,13*Z*,9′*Z*)		+
22	(7*Z*,9*Z*,7′*Z*,9′*Z*)	+	+
23	(7*Z*,9*Z*,11*Z*,7′*Z*,9′*Z*)		+

((13*Z*)) and presumably **14** ((9*Z*)) were isolated from the ripe hips of *Rosea pomifera*; UV/VIS and ^{1}H-NMR data are specified for **15** [21].

We now wish to report on the synthesis of the five (*Z*)-isomers **13** ((7*Z*)), **17** ((7*Z*,7′*Z*)), **18** ((9*Z*,9′*Z*)), **19** ((7*Z*,9*Z*,7′*Z*)), and **22** ((7*Z*,9*Z*,7′*Z*,9′*Z*); *Table 1*). The symmetrical isomers **17**, **18**, and **22** were prepared by double *Wittig* condensation of the phosphonium salt **4**, **7**, or **6**, respectively, with the C_{10}-dialdehyde **8** [9] in refluxing EtOH with 1,2-epoxybutane or NaOMe (for **22**) as acid scavenger. The yields of pure (> 96% HPLC) isomers varied from 43 to 52%.

On the other hand, the synthesis of the asymmetric isomers **13** and **19** had to follow a stepwise $C_{10} \rightarrow C_{25} \rightarrow C_{40}$ sequence principle *via* (7*Z*)-zeaxanthinal **10**. In the case of the (tri-*Z*)-isomer **19**, this approach proved somewhat more efficient than using the (di-*Z*)-zeaxanthinal **12**, where only inseparable mixtures were obtained. Yields (13–46%) and purities (93–97%) were somewhat lower. In this fashion, zeaxanthin isomers with (7*Z*)-configuration were specifically synthesized for the first time. Detailed spectroscopic data are discussed below.

3. Isolation of Isomers. – A series of eleven (*Z*)-isomeric zeaxanthins was isolated from various synthetic mixtures using HPLC methods (*Table 1*). Though more efficient

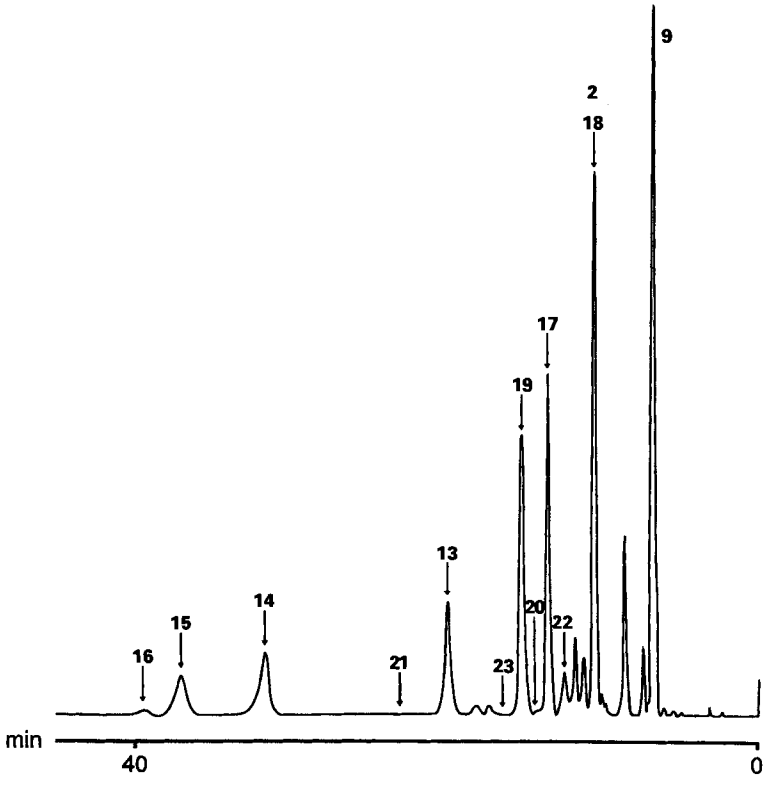

Figure. *HPLC of an artificial mixture of* (Z,E)*-zeaxanthins demonstrating the achieved separation according to* Method 1 (see *Exper. Part*)

separation procedures are known today, our results appear sufficiently interesting to be presented here. Most isomers were well separated on *Spherisorb S5W* (*Method 1*). However, for the separation of **2** ((all-*E*)) and **18** ((9*Z*,9′*Z*)), *Lichrosorb SI 60* (*Method 2*) had to be used. The latter system, on the other hand, did not separate **17** ((7*Z*,7′*Z*)), **18** ((9*Z*,9′*Z*)), and **19** ((7*Z*,9*Z*,7′*Z*)). A typical chromatogram is shown in the *Figure*.

4. Discussion of ^{1}H-NMR Data. – All compounds in this investigation were fully characterized by ^{1}H-NMR. The data of compounds **6–12** (except **8**) are given in the *Exper. Part.*

In *Tables 2* and *3* are collected the chemical shifts of **2** ((all-*E*)) and its (*Z*)-isomers **13–23**. The coupling constants are not specifically quoted, since they were found in the expected range, namely $J(7,8)$ = *ca.* 16.5 ((*E*)) and *ca.* 12.5 ((*Z*)), $J(10,11)$ = *ca.* 11.3–12, and $J(11,12)$ = *ca.* 14.8 ((*E*)) and 12.2 Hz ((*Z*)). It is clearly evident that the configuration at C(7,7′) and C(11,11′) can unambiguously be deduced from these coupling constants.

It has previously been demonstrated that ^{1}H-NMR at higher magnetic fields is an extremely efficient technique for the elucidation of the structure of (*Z*)-isomeric carotenoids [22]. From a study of the spectra of more than 40 isomers from seven types of C_{40} carotenoids, it was shown that the so-called isomerization shift $\Delta\delta$ (in ppm), *i.e.* the shift difference $\delta(Z) - \delta(E)$ of the different protons, is very characteristic and indicative for the position of the stereomutated bond(s). A few simple rules derived from this study helped to readily deduce the structure of nine (*Z*)-isomers of astaxanthin diacetate [23] and of eight (*Z*)-isomers of β,β-carotene [24]. Therefore, relevant $\Delta\delta$ values (> 0.02 ppm) for isomers **13–23** are given in *Tables 2* and *3*, and the proposed structures are mainly based upon these values.

Thus, (9*Z*)- and (13*Z*)-stereomutation were evidenced by a strong downfield shift of H–C(8) and H–C(12), respectively, of *ca.* 0.5 ppm. A (7*Z*)-isomerization was reflected by the reduction of $J(7,8)$ and, moreover, by relevant $\Delta\delta$ values of $CH_3(19)$ and $CH_3(18)$. This points to a strong steric interaction of both groups of protons. Stereomutation of C(15)=C(15′) is readily detected from an interchange of the relative position of the signals of H–C(14,14′) and H–C(15,15′). The former can be distinguished from the latter since they were broadened by a normally unresolved broadening by allylic coupling to $CH_3(20,20')$.

Close inspection of the $\Delta\delta$ values in *Tables 2* and *3* (see also [22–24]) indicates that separated (*Z*)-bonds behave fairly additive. This considerably simplified the assignments. As an example, the chemical shifts of the (9*Z*,13*Z*,9′*Z*)-isomer **21** can be fairly well predicted from the $\Delta\delta$ values of the (9*Z*)- and (13*Z*)-isomers. As expected, additivity fails if successive bonds were stereomutated, although some gross features were always retained as expected.

In all cases, the assignments and hence the elucidation of the structure of the isomers were straightforward, and most of the protons were detected despite some strong overlap. Only in a few cases, decisive decoupling experiments were required. In addition, isomers **13**, **19**, and **22** were subjected to some steady-state NOE difference experiments which fully corroborated the proposed structures.

A few remarks on the spectra of isomers with highly sterically hindered (7*Z*)-bonds should be added here. It has been shown previously [25] [26] that retinals and related smaller model compounds with (7*Z*)-geometry show temperature-dependent ^{1}H-NMR

spectra. Particularly the signal of $CH_3(16)$ and $CH_3(17)$ changed upon cooling to *ca.* −60° from a sharp *s* to 2 *s*. From the coalescence temperature and the shift difference of the 2 *s*, the free energy of activation ΔG^+ was estimated to be between *ca.* 11 and 20 kcal/mol [26]. This temperature-dependence was explained by the assumption that rotation around the C(6)–C(7) bond was highly hindered in these (7*Z*)-isomers. These rotational isomers are, therefore, enantiomeric.

Table 2. *^{1}H-NMR Data for (all-*E*)- and Four (mono-*Z*)-isomers of Zeaxanthin.* δ in ppm; shift differences $\Delta\delta = \delta(Z) - \delta(E)$ for absolute values > 0.02 ppm; at 270 or 400 MHz in $CDCl_3$, 26°; n.r. = not resolved, br. = broad.

	2 ((all-*E*))[a]	**13** ((7*Z*))[a]		**14** ((9*Z*))[b]		**15** ((13*Z*))[a]		**16** ((15*Z*))[b]	
	δ	δ	$\Delta\delta$	δ	$\Delta\delta$	δ	$\Delta\delta$	δ	$\Delta\delta$
H_{ax}–C(2)	1.48	1.51	0.03	1.51	0.03	1.49		1.48	
H_{ax}–C(2′)		1.48		1.47		1.48			
H_{eq}–C(2)	1.77	*ca.* 1.77		n.r.		*ca.* 1.78		1.78	
H_{eq}–C(2′)		*ca.* 1.77		n.r.		*ca.* 1.78			
H_{ax}–C(3)	*ca.* 4.00	*ca.* 4.01		*ca.* 4.01		*ca.* 4.01		*ca.* 4.00	
H_{ax}–C(3′)									
H_{ax}–C(4)	2.04	n.r.		2.07	0.03	*ca.* 2.04		2.05	
H_{ax}–C(4′)		n.r.		2.07		*ca.* 2.04			
H_{eq}–C(4)	2.39	2.35	−0.04	2.42	0.03	*ca.* 2.39		2.39	
H_{eq}–C(4′)		2.39		2.38		*ca.* 2.39			
H–C(7)	6.11	5.79 (br.)	−0.32	6.12		*ca.* 6.13		6.10	
H–C(7′)		6.11		6.12		6.12			
H–C(8)	6.13	*ca.* 6.13		6.67	0.54	*ca.* 6.14		6.14	
H–C(8′)		6.13		*ca.* 6.12		6.13			
H–C(10)	6.16	6.22	0.06	6.07	−0.09	6.20	0.05	6.16	
H–C(10′)		6.16		6.16		6.16			
H–C(11)	6.64	6.57	−0.08	6.74	0.10	6.63		6.68	0.04
H–C(11′)		6.64		6.64		6.64			
H–C(12)	6.36	6.33	−0.03	6.30	−0.06	6.86	0.51	6.43	0.07
H–C(12′)		6.36		6.37		6.36			
H–C(14)	*ca.* 6.26	*ca.* 6.25		*ca.* 6.25		6.11	−0.15	6.66	0.41
H–C(14′)				*ca.* 6.25		6.23			
H–C(15)	*ca.* 6.63	*ca.* 6.63		*ca.* 6.64		6.79	0.16	6.40	−0.23
H–C(15′)						6.56	−0.07		
$CH_3(16)$	1.074	[c]		1.083		1.080		1.077	
$CH_3(17)$				1.092					
$CH_3(16')$	1.074	1.074		1.074		1.074		1.077	
$CH_3(17')$									
$CH_3(18)$	1.736	1.556	−0.18	1.776	0.04	1.743		1.745	
$CH_3(18')$		1.736		1.738		1.736			
$CH_3(19)$	1.967	1.856	−0.11	*ca.* 1.969		1.964		1.977	
$CH_3(20)$	1.972	1.957		*ca.* 1.969		1.993			
$CH_3(19')$	1.967	1.967		*ca.* 1.969		1.964		1.977	
$CH_3(20')$	1.972	1.971		*ca.* 1.969		1.973			
OH–C(3)	*ca.* 1.35	*ca.* 1.36 (br.)		*ca.* 1.41		*ca.* 1.41		1.37	
OH–C(3′)									

[a]) At 400 MHz.
[b]) At 270 MHz.
[c]) Temperature-dependent broad signals. Peaks or shoulders visible at 1.084, 1.093, 1.101, and 1.109 ppm; see text.

Table 3. *^{1}H-NMR data for Two (di-Z)-, Three (tri-Z)-, One (tetra-Z)-, and One (penta-Z)-Isomers of Zeaxanthin.* δ in ppm; shift differences $\Delta\delta = \delta(Z) - \delta(E)$ for absolute values > 0.02 ppm; at 400 MHz in $CDCl_3$, 26°; n.r. = not resolved, br. = broad.

Proton	**17** ((7Z,7'Z))		**18** ((9Z,9'Z))		**19** ((7Z,9Z,7'Z))		**20** ((7Z,11Z,7'Z))		**21** ((9Z,13Z,9'Z))		**22** ((7Z,9Z,7'Z,9'Z))		**23** ((7Z,9Z,11Z,7'Z,9'Z))	
	δ	$\Delta\delta$	δ	$\Delta\delta$	δ	$\Delta\delta$	δ	$\Delta\delta$	δ	$\Delta\delta$	δ	$\Delta\delta$	δ	$\Delta\delta$
H_{ax}–C(2)	1.50		1.50		1.48		n.r.		1.50		1.48		1.48	
H_{ax}–C(2')					1.50		n.r.		1.50				1.48	
H_{eq}–C(2)	1.80	0.03	1.79		n.r.		n.r.		1.79		1.79		1.79	
H_{eq}–C(2')					n.r.		n.r.		1.79				1.79	
H_{ax}–C(3)	*ca.* 4.03	0.03	*ca.* 4.03	*ca.* 0.03	*ca.* 4.02		*ca.* 4.02		*ca.* 4.03	*ca.* 0.03	*ca.* 4.01		*ca.* 4.01	
H_{ax}–C(3')														
H_{ax}–C(4)	1.99	−0.05	2.07	0.03	*ca.* 1.99	*ca.* −0.05	n.r.		2.07	0.03	1.98	−0.06	1.99	−0.05
H_{ax}–C(4')					*ca.* 1.99	*ca.* −0.05	n.r.		2.07	0.03			1.99	−0.05
H_{eq}–C(4)	2.35	−0.03	2.42	0.03	*ca.* 2.35	*ca.* −0.03	*ca.* 2.34		2.41		2.35	−0.03	2.35	−0.03
H_{eq}–C(4')					*ca.* 2.35	*ca.* −0.03	*ca.* 2.34		2.41				2.35	−0.03
H–C(7)	5.78 (br.)	−0.33	6.12		5.94 (br.)	−0.17	*ca.* 5.79 (br.)	*ca.* −0.32	6.14	0.03	5.94 (br.)	−0.17	5.97 (br.)	−0.14
H–C(7')					5.78	−0.34			*ca.* 6.12				5.94 (br.)	−0.17
H–C(8)	6.13		6.66	0.53	6.62	0.49	6.13		6.66	0.53	6.62	0.49	6.57	0.44
H–C(8')					6.13		6.13		6.66	0.53			6.62	0.49
H–C(10)	6.22	0.06	6.07	−0.09	6.01	−0.15	6.73	0.57	*ca.* 6.12 (?)	−0.04 (?)	6.00	−0.15	6.48	0.33
H–C(10')					6.21	0.06	6.22	0.06	6.07	−0.09			6.01	−0.15
H–C(11)	6.56	−0.08	6.73	0.09	6.67	0.03	6.24	−0.41	6.73	0.09	6.67	0.03	6.31	−0.33
H–C(11')					6.56	−0.08	6.56	−0.08	6.72	0.08			6.66	
H–C(12)	6.33	−0.04	6.29	−0.07	6.26	−0.10	5.97	−0.39	6.82	0.46	6.26	−0.10	5.90	−0.46
H–C(12')					6.32	−0.04	6.32	−0.04	6.29	−0.07			6.26	−0.10

Table 3 (cont.)

Proton	**17** ((7Z,7′Z))		**18** ((9Z,9′Z))		**19** ((7Z,9Z,7′Z))		**20** ((7Z,11Z,7′Z))		**21** ((9Z,13Z,9′Z))		**22** ((7Z,9Z,7′Z,9′Z))		**23** ((7Z,9Z,11Z,7′Z,9′Z))	
	δ	$\Delta\delta$	δ	$\Delta\delta$	δ	$\Delta\delta$	δ	$\Delta\delta$	δ	$\Delta\delta$	δ	$\Delta\delta$	δ	$\Delta\delta$
H–C(14)	*ca.* 6.25		*ca.* 6.24		*ca.* 6.25		*ca.* 6.28		*ca.* 6.12(?)	−0.14(?)	*ca.* 6.23		*ca.* 6.24	
H–C(14′)							*ca.* 6.25		6.22	−0.03				
H–C(15)	*ca.* 6.62		*ca.* 6.62		*ca.* 6.62		*ca.* 6.61		6.78	0.15	*ca.* 6.62		*ca.* 6.62	
H–C(15′)									6.54	−0.09				
CH_3(16)	[a]		1.083		1.097		[c]		1.085		1.097		1.100	0.03
CH_3(17)			1.093		1.108	0.03			1.094		1.108	0.03	1.110	0.04
CH_3(16′)	[a]		1.083		[b]		[c]		1.085		1.097		1.100	0.03
CH_3(17′)			1.093						1.094		1.108	0.03	1.110	0.04
CH_3(18)	1.556	−0.18	1.773	0.04	1.514	−0.22	*ca.* 1.559	−0.18	1.772	0.04	1.514	−0.22	*ca.* 1.527	−0.21
CH_3(18′)					1.555	−0.18	*ca.* 1.559	−0.18	1.772	0.04			*ca.* 1.527	−0.21
CH_3(19)	1.856	−0.11	1.967		1.802	−0.17	1.836	−0.13	1.983		1.802	−0.17	1.816	−0.15
CH_3(20)	1.957				*ca.* 1.956		2.073	0.10	1.978		1.955		2.071	0.10
CH_3(19′)	1.856	−0.11	1.958		1.855	−0.11	1.856	−0.11	1.968		1.802	−0.17	1.803	−0.16
CH_3(20′)	1.957				*ca.* 1.956		1.955		1.949		1.955		1.956	
OH–C(3)	1.37		1.39		1.37		1.33		1.36		*ca.* 1.34 (br.)		*ca.* 1.34 (br.)	
OH–C(3′)					1.35		1.35		1.36					

[a] Group of broad signals between *ca.* 1.08 and 1.11 ppm; peaks at 1.087 and 1.099 ppm.

[b] Broad signal between *ca.* 1.08 and 1.11 ppm.

[c] Partly broadened signals, peaks at 1.087, 1.102, and 1.110 ppm.

In 3-substituted compounds such as zeaxanthin, on the other hand, the half-chair conformation with equatorial OH group is clearly preferred as evidenced by the line-width of the H_{ax}–C(3) signal. Thus, molecules with high steric hindrance due to (7*Z*) and an (unsymmetrical) orientation of the side-chain above and below the ring are diastereoisomers. They are expected to be ^{1}H-NMR-spectroscopically distinguishable, if their rate of interconversion is sufficiently slow. Evidence for this behaviour was clearly visible here in the spectra of those isomers having at least one isolated (7*Z*)- or (7′*Z*)-bond (**13**, **17**, and **20**). In all these cases, the signals of the geminal Me groups at C(1) (or C(1′)) and those of H–C(7) (or H–C(7′)) close to the (7*Z*)-bond were considerably broader at room temperature. In the spectra of isomers with (7*Z*,9*Z*)-bonds (**19**, **22**, and **23**), on the other hand, the signals of the geminal Me groups at C(1) were sharp indicating a more rapid interconversion. In order to support this view, some experiments at variable temperature were performed with isomers **13**, **17**, and **19**.

In the ^{1}H-NMR spectrum of **13** ((7*Z*)) at 26° (at 400 MHz, $CDCl_3$), the signal of CH_3(16′) and CH_3(17′) were observed as a common sharp *s* at 1.074 ppm as in (all-*E*)-isomer **2**; this is interpreted as being an accidental equivalency (see below). The signals of CH_3(16) and CH_3(17), on the other hand, consisted of a broad hump between *ca.* 1.07 and 1.11 ppm with at least three maxima at 1.084, 1.093, 1.101, and one shoulder at 1.109 ppm due to the two diastereoisomeric species. In addition, the *d* of H–C(7) had a considerably larger line-width than that of H–C(7′).

Upon cooling down to *ca.* –60°, the spectrum revealed a doubling (1:1 intensities) of several further signals due to the presence of conformationally 'frozen' diastereoisomers, *e.g.* at 1.857 and 1.822 ppm (CH_3(19)), at 1.548 and 1.500 ppm (CH_3(18)), at 5.81 and 5.79 ppm (still broad *d* of H–C(7)), *etc.* The signals around 1.1 ppm of the geminal Me groups at C(1) and C(1′) can be assigned in the following way: 1.155, 1.134, 1.063, and 1.044 ppm (together *ca.* 6 H) are attributed to the 2 nonequivalent Me groups at C(1) (CH_3(16), CH_3(17)) of the two diastereoisomers. Two further signals at 1.063 and 1.083 ppm (together 6 H) are assigned to the Me groups attached to C(1′) (CH_3(16′), CH_3(17′)). Here, the accidental shift equivalency observed at 26° is removed at lower temperatures. It is obvious that the presence of diastereoisomeric pairs of sterically hindered optically active (7*Z*)-zeaxanthins will strongly influence the CD properties of these compounds (see below).

With (7*Z*,7′*Z*)-**17**, warming up to 45° resulted in a sharpening of some signals, especially of the Me groups at C(1) and C(1′). However, since part of the sample clearly stereomutated, the results were so far not completely understood. Similar stability problems were encountered with **19**. It is clear from these preliminary experiments that a full interpretation and quantitative evaluation of the temperature-dependent spectra would need more detailed experimental and theoretical studies.

5. Discussion of CD Data. – A large number of carotenoids show a characteristic system of nine C=C bonds formally conjugated with a C(5)=C(6) bond in the ring system. Their chirality is believed to originate from distortion of the whole conjugated system by a twist around the C(6)–C(7) bond. That twist is caused by sterical interference of H–C(8) with either CH_3(18) or CH_3(16), CH_3(17). The OH substituent at the asymmetric center C(3) determines the most favorable ring conformation (OH equatorial as determined by ^{1}H-NMR) and, therefore, also the sense of the twist and the dihedral angle of the C(6)–C(7) bond, thus creating a so-called intrinsically chiral chromophore [20]. A (*Z*)-arrangement at one of the 'unhindered' (*Z*)-bonds distant from the end-group ring, such as in (9*Z*)-, (13*Z*)-, or (15*Z*)-isomers, has no significant sterical influence on the C(6)–C(7) bond. However, sterical hindrance with CH_3(19) is increased extremely in the case of (7*Z*)-compounds. A (*Z*)-stereomutation in the middle of the backbone ((15*Z*)-zeaxanthin) tilts the symmetry axis of the molecule with respect to the plane of the conjugated system. As a result, the CD spectrum is inverted. The relative intensities of the 4 maxima in the range 400–200 nm are, however, altered. At the so-called '*cis*-peak' (*ca.*

340 nm), the maximum intensity is high in (15*Z*)-zeaxanthin (**16**) [20], while it is relatively weak in the (all-*E*)-isomer **2**.

In the past, the CD spectra of several 'unhindered' (mono-*Z*)- and (di-*Z*)-isomers of zeaxanthin have been reported; *i.e.* of (9*Z*)- and (13*Z*)-isomers **14** and **15**, respectively [17], and of (15*Z*)- and (9*Z*,9′*Z*)-isomers **16** and **18**, respectively [20]. The present complementary data will allow to deduce the influence on the CD spectra of a given (*Z*)-double bond as well as of (poly-*Z*)-configurations in the chain. We will first discuss the influence of the position of a single (*Z*)-bond by comparing the symmetrical (15*Z*)-isomer **16** and the (13*Z*)-, (9*Z*)-, and (7*Z*)-isomers **15**, **14**, and **13**, respectively, with the (all-*E*)-isomer **2**. Second, the two symmetrical (di-*Z*)-isomers **18** ((9*Z*,9′*Z*)) and **17** ((7*Z*,7′*Z*)) are compared with **2**. Finally, we will discuss the CD spectra of the (tri-*Z*)-, (tetra-*Z*)-, and (penta-*Z*)-isomers (see *Table 4* for the details).

Table 4. *Positions and Relative Intensities of the CD Peaks* (in EPA) *in the Near-UV Region*[a])

	Temp.	$\lambda_5(\Delta\varepsilon_5)$	$\lambda_4(\Delta\varepsilon_4)$	$\lambda_3(\Delta\varepsilon_3)$	$\lambda_2(\Delta\varepsilon_2)$
(all-*E*) **2**	25°	222 (−1.39)	247 (1.0)	284 (−1.96)	341 (0.39)
(mono-*Z*)					
14 ((9*Z*))	25°	223 (0.42)	249 (−1.0)	288 (0.64)	343 (−0.49)
15 ((13*Z*))	25°	211 (1.47)	243 (−1.0)	285 (1.52)	338 (−1.91)
16 ((15*Z*))	25°	220 (0.57)	242 8−1.0)	284 (1.49)	338 (−2.55)
13 ((7*Z*))	25°	220 (1.7)	245 (−1.0)	280 (−0.96)	340 (−0.21)
	−60°	220 (1.4)	245 (−1.0)	280 (−0.1)	344 (−0.36)
	−180°	225 (1.29)	247 (−1.0)	280 (−0.2)	350 (−0.3)
(di-*Z*)					
18 ((9*Z*,9′*Z*))	25°	225 (−1.71)	248 (1.0)	288 (−1.15)	340 (0.57)
17 ((7*Z*,7′*Z*))[b])	25°	213 (0.5)	236 (−1.0)	276 (0.5)	357 (0.2)
			260 (sh)		
(poly-*Z*)					
19 ((7*Z*,9*Z*,7′*Z*))	25°	245 (0.7)	269 (1.2)		343 (0.4)
	−90°	235 (3.2)	245 (sh)	266 (0.7)	340 (1.1, br.)
20 ((7*Z*,11*Z*,7′*Z*))	25°				335 (1.0, br.)
	−180°	241 (1.4)	280 (−0.8)	335 (sh)	350 (1.7)
22 ((7*Z*,9*Z*,7′*Z*,9′*Z*))	25°	225 (2.9)	245 (−0.7)	275 (1.3, br.)	*ca.* 3.10 (0.7 br.)
					340 (−0.4)
	−150°	220 (11.0)	240 (−4.8)	275 (3.5, br.)	328 (−2.8)
					342 (−4.1)
23 ((7*Z*,9*Z*,11*Z*,7′*Z*,9′*Z*))	25°	*ca.* 260 (2.0, v. br.)		305 (0.8)	
	−120°	244 (5.5)	282 (−1.2)	305 (0.8)	332 (−0.5)
					345 (−0.7)

[a]) EPA = Et_2O/isopentane/EtOH 5:5:2; sh = shoulder, br. = broad, v. br. = very broad.
[b]) Mean values from different spectra, values only approximate.

(Mono-Z)-Isomers **13**–**16**. *Table 4* summarizes the positions and relative intensities of the four maxima λ_2 to λ_5 of **13**–**16** in the spectral range 400–200 nm. The intensities are normalized with respect to the maximum at *ca.* 250 nm (λ_4), since the absolute intensities could be susceptible to erroneous concentrations.

The three unhindered (mono-*Z*)-isomers **14**–**16** have their signs reversed with respect to the (all-*E*)-isomer **2**. Again, the (9*Z*,9′*Z*)-isomer **18** shows the same signs as **2**. The CD at the so-called '*cis*-peak' around 340 nm (λ_2) increases strongly as the (*Z*)-bond 'moves'

towards the center of the molecule. In the (all-*E*)- and the (9*Z*)-isomers, the '*cis*-peak' has a similar relative intensity. The maximum at 280 nm (λ_3) changes its relative intensity in a rather irregular way. The spectra of the unhindered (9*Z*)-, (13*Z*)-, and (15*Z*)-isomers **14**–**16** look quite similar; the peaks are alternating regularly in sign at progressing wavelength, although their relative intensities change substantially.

The (7*Z*)-isomer **13**, instead, differs in shape and temperature dependence of its CD spectrum from other (*Z*)-isomers. The spectra of the three unhindered isomers **14**–**16** increase regularly in intensity upon cooling; the relative intensities are only weakly affected. The CD of **13** at room temperature looks quite different from those of **14**–**16**, the regular sign alternation being lost due to a negative maximum around 280 nm. Upon cooling, the peaks sharpen, most intensities increase tremendously, only the negative maximum around 280 nm disappears almost completely, and the spectrum becomes quite similar to the ones of **14**–**16**, with the exception of the latter peak.

(Di-Z)-Isomers **18** *and* **19**. In this series, only the (9*Z*,9′*Z*)- and (7*Z*,7′*Z*)-isomers were available. The CD spectrum of the (9*Z*,9′*Z*)-compound **18** resembles that of the (all-*E*)-isomer **2**, but is opposite to the (9*Z*)-isomer **14**. The (7*Z*,7′*Z*)-compound **17**, on the other hand, is quite different. Its spectrum is not opposite to the (7*Z*)-isomer **13**. Unfortunately, due to the instability of **17**, the spectrum is not very accurate; at low temperature, the shoulder at 260 nm becomes weaker and the positive maximum at 213 nm turns into a negative maximum between the strong negative maxima at 236 and 210 nm. This effect again shows that a (7*Z*)-bond has a distinctly different influence on the CD spectrum as compared with other (*Z*)-bonds more distant from the ring: while the (7*Z*)-arrangement changes the relationship backbone-ring dramatically, the introduction of (*Z*)-bonds more distant from the ring does not influence the sterical backbone-ring relation; it only changes the overall symmetry of the molecule and the conjugation of the backbone itself. This results in a *cis*-shift of the main absorption band, an enhanced extinction coefficient of the '*cis*-peak' in the absorption spectrum, and the change of the relative intensities and signs of the CD maxima.

(Poly-Z)-Isomers **19**, **20**, **22**, *and* **23**. Their CD spectra are rather diffuse at room temperature, but they sharpen considerably at low temperature and become more intense, some maxima even change sign (see *Table 4*). Unfortunately, it seems not possible to extract much regularity from the data. Comparison of the shape of the CD curves shows that the two (tri-*Z*)-isomers **19** and **20** exhibit quite similar spectra. They are, however, neither equal to nor a mirror image of the (7*Z*,7′*Z*)-isomer **17**. The (tetra-*Z*)- and (penta-*Z*)-isomers **22** and **23**, respectively, have also quite different CD curves: while the positions of the maxima are similar, the signs are not.

6. Discussion of UV/VIS Data. – *Table 5* summarizes the measured absorption maxima and molar extinction coefficients of **2** and **13**–**23**. From the VIS absorption around 440 nm, only the most intense one of the three vibrational components is given. Also included are absorption values around 340 nm ('*cis*-peak') and for the rather weak maximum at *ca.* 270 nm. The latter absorption corresponds to a strong maximum in the CD spectrum. In addition, relative intensities of '*cis*-peak' and maximum absorption ($\varepsilon_2/\varepsilon_1$) are cited.

Some regularities can be deduced from *Table 5*: All maxima including the '*cis*-peak' are shifted sligthly towards shorter wavelengths with increasing number of (*Z*)-bonds.

Table 5. *UV/VIS Maxima and Relative Absorption Intensities* (in EPA)[a])

	$\lambda_3(\varepsilon_3)$	$\lambda_2(\varepsilon_2)$	$\lambda_1(\varepsilon_1)$	$\varepsilon_2/\varepsilon_1$
(all-*E*) **2**	273 (22000)	340 (7300)	450 (139300)	0.053
(mono-*Z*)				
13 (7*Z*)	267 (10500)	334 (5500)	447 (61200)	0.089
14 (9*Z*)	260 (11500)	340 (9500)	444 (84400)	0.112
15 (13*Z*)	275 (17200)	337 (26400)	447 (113300)	0.233
16 (15*Z*)	277 (11600)	336 (43200)	446 (71000)	0.603
(di-*Z*)				
17 (7*Z*,7′*Z*)	266 (9900)	334 (3700)	445 (64000)	0.058
18 (9*Z*,9′*Z*)	270 (16000)	340 (11400)	440 (122300)	0.093
(poly-*Z*)				
19 (7*Z*,9*Z*,7′*Z*)	263 (13200)	330 (7200)	438 (121600)	0.059
20 (7*Z*,11*Z*,7′*Z*)	267 (10100)	334 (11000)	442 (54400)	0.202
21 (9*Z*,13*Z*,9′*Z*)		340 (7300)	432 (57000)	0.128
22 (7*Z*,9*Z*,7′*Z*,9′*Z*)	260 (13200)	330 (7000)	433 (119400)	0.058
23 (7*Z*,9*Z*,11*Z*,7′*Z*,9′*Z*)	260 (22800)	330 (13500)	435 (73200)	0.184

[a]) EPA = Et_2O/isopentane/EtOH 5:5:2.

The shift from the (all-*E*)- (**2**) to the (penta-*Z*)-isomer **23** is 15 nm for the strongest maximum and 10 nm for the '*cis*-peak'.

The extinction coefficient ε_1 of the λ_1 maximum is higher for **2** than for the (*Z*)-isomers. The position of the (*Z*)-bond in the chain does not seem to result in a regular trend. Unexpected high absorption values are measured, however, for the (13*Z*)-, (9*Z*,9′*Z*)-, and (7*Z*,9*Z*,7′*Z*)-isomers **15**, **18**, and **19**, respectively.

The intensity ratios $\varepsilon_2/\varepsilon_1$ depend strongly on the position of the (*Z*)-bond in the chain. Values are smallest for the (*E*)-isomer **2** and highest for the (15*Z*)-isomer **16**. A similar trend is observed for the (di-*Z*)-isomers, where (9*Z*,9′*Z*) > (7*Z*,7′*Z*). For the (tri-*Z*)-isomers, the situation is more complex; highest values are observed for the (7*Z*,11*Z*,7′*Z*)-isomer **20**, lowest values for the (7*Z*,9*Z*,7′*Z*)-isomer **19**.

We would like to thank all the colleagues who helped us in carrying out this work. Special thanks are due to *W. Arnold*, *W. Meister*, *F. Kachler*, and *A. Dirscherl* †.

Experimental Part

General. HPLC separations: 50 × 0.31 cm columns; *Method 1: Spherisorb S5W*, silica *B 13/255*, hexane/CH_2Cl_2 (6.5%)/i-PrOH (2.5%) and *Hünig*'s base (0.1%); *Method 2*: *Lichrosorb SI 60* (5 μm) instead of *Spherisorb*. UV/VIS spectra: *Beckman DK-2A*; λ_{max} ($E_{1cm}^{1\%}$) in nm at r.t.; $CHCl_3$ or EPA (Et_2O/isopentane/EtOH 5:5:2). CD spectra: dichrographe *Mark II* (*Jobin-Yvon*) fitted with a 450-W Xe arc and an automatic scan control for repetitive scanning and accumulation on an on-line *DEC 11/23* computer for data reduction (smoothing, background subtraction *etc.*); in EPA; variable-temperature cell of a commercial type (*Jobin-Yvon*). ^{1}H-NMR spectra: *Bruker-HX-270-FT* (270 MHz) or *Bruker-WM-400* and *AM-400-FT* spectrometer (400 MHz); in $CDCl_3$ at *ca.* 26° with TMS as internal standard; for **20**, **21**, and **23**, only *ca.* 50–100 μg were available; in all other cases, quantities in the mg range with *ca.* 0.5 ml of solvent were used; carotenoid numbering.

1. *{(2Z,4Z)-5-[(R)-4-Hydroxy-2,6,6-trimethylcyclohex-1-enyl]-3-methylpenta-2,4-dienyl}triphenylphosphonium Chloride* (**6**). A slurry of *Raney*-Ni (58 g; *Degussa*, type *B 113 W*) and 2,2′-(ethylenedithio)bis[ethanol] (0.65 g) in MeOH (0.8 l) was prehydrogenated at 30°/1 bar H_2 for 0.5 h. The phosphonium salt (9*Z*)-**3** (200 g, 0.388 mol) in

MeOH (1.1 l) was added and hydrogenation carried out at 30°/1 bar H_2 until uptake of H_2 ceased (11 h). The catalyst was removed by filtration and washed with MeOH (0.3 l). The product was crystallized by concentration of the filtrate *in vacuo* to *ca.* 340 g, followed by slow addition of AcOEt (6 l) and stirring the suspension at 0° over night. The white crystals were further purified by recrystallization from MeOH (0.17 l) and AcOEt (3 l) at r.t. The crystals were washed with AcOEt/MeOH 98:2 (0.5 l) and dried at 50°/0.01 mbar for 24 h: 145.8 g (68.3%) of **6**. White crystals. M.p. 114–116°. $[\alpha]_D^{20} = -20.4$ ($c = 1$, $CHCl_3$). HPLC: 99.2%. UV (EtOH): 268 (264), 275 (241). IR (KBr): 3342*s*, 3320*s*, 1585*w*, 1484*w*, 1437*s*, 1111*s*, 1040*s*, 739*s*, 691*s*. ^{1}H-NMR (400 MHz, $CDCl_3$): 7.3–7.9 (*m*, 15 arom. H); 6.07 (*d*, $J = 12.6$, H–C(7)); 5.90 (*d*, $J = 12.6$, H–C(8)); 5.14 (br. *dt*, $J = 4.8$, 8.2, H–C(10)); 4.74 (br. *ddd*, $J = 15.8$, 15.6, 8.2, H–C(11)); 4.69 (br. *ddd*, $J = 15.8$, 15.6, 8.2, H–C(11)); 3.91–4.02 (*m*, H–C(3)); 3.44 (*s*, MeOH); 2.90 (br. *s*, OH–C(3)); 2.31 (*dd*, $J = 17.0$, 5.5, H_{eq}–C(4)); 2.00 (*dd*, $J = 17.0$, 9, H_{ax}–C(4)); 1.73 (*ddd*, $J = 12.2$, 3, 2, H_{eq}–C(2)); 1.69 (*d*, $J = 4.8$, Me–C(9)); 1.45 (*dd*, $J = 12.2$, 11.6, H_{ax}–C(2)); 1.29 (*s*, Me–C(5)); 0.98 (*s*, 1 Me–C(1)); 0.94 (*s*, 1 Me–C(1)). FAB-MS (3-nitrobenzyl alcohol): 481 (100, M^+), 391 (5), 307 (18), 289 (10), 275 (8), 202 (35), 183 (13), 154 (82), 136 (59). Anal. calc. for $C_{33}H_{38}ClOP \cdot MeOH$ (549.14): C 74.31, H 7.83, Cl 6.46; found: C 74.37, H 7.71, Cl 6.46.

2. *{(2Z,4E)-5-[(R)-4-Hydroxy-2,6,6-trimethylcyclohex-1-enyl]-3-methylpenta-2,4-dienyl}triphenylphosphonium Chloride* (**7**). A soln. of **6** (134 g, 0.259 mol) and $Pd(OAc)_2$ (134 mg) in MeOH (1.3 l) was stirred at 65° under Ar for 4 h. The orange soln. was concentrated *in vacuo* to 230 g. AcOEt (4.3 l) was slowly added and the suspension stirred at r.t. for 3 h. The white crystals were washed with AcOEt (0.5 l), then recrystallized in a similar way from MeOH (0.1 l) and AcOEt (3.7 l), and dried at 50°/0.01 mbar for 48 h: 115.6 g (86.3%) of 7. White crystals. M.p. 195–196°. $[\alpha]_D^{20} = -53.2$ ($c = 1$, $CHCl_3$). HPLC: 99.5%. UV (EtOH): 268 (288), 275 (289). IR (KBr): 3287*s*, 1585*w*, 1485*w*, 1438*s*, 1111*s*, 1055*s*, 747*s*, 691*s*. ^{1}H-NMR (400 MHz, $CDCl_3$): 7.6–7.9 (*m*, 15 arom. H); 6.12 (*d*, $J = 15.8$, H–C(7)); 5.93 (*d*, $J = 15.8$, H–C(8)); 5.30 (br. *dt*, $J = 5.4$, 8.2, H–C(10)); 4.8 (br. *ddd*, $J = 16.9$, 15.6, 8.2, 2 H–C(11)); 3.88–4.00 (*m*, H–C(3)); 2.77 (br. *s*, OH–C(3)); 2.33 (*dd*, $J = 16.9$, 5.4, H_{eq}–C(4)); 1.99 (*dd*, $J = 16.9$, 9.5, H_{ax}–C(4)); 1.86 (*d*, $J = 5.4$, Me–C(9)); 1.72 (*ddd*, $J = 12.2$, 3, 2, H_{eq}–C(2)); 1.41 (*dd*, $J = 12.2$, 11.8, H_{ax}–C(2)); 1.39 (*s*, Me–C(5)); 0.892 (*s*, 1 Me–C(1)); 0.887 (*s*, 1 Me–C(1)). FAB-MS (3-nitrobenzyl alcohol): 481 (100, M^+), 307 (12), 289 (9), 275 (7), 202 (44), 183 (14), 154 (63), 136 (58). Anal. calc. for $C_{33}H_{38}ClOP$ (517.09): C 76.65, H 7.41, Cl 6.86; found: C 76.73, H 5.56, Cl 6.87.

3. *(all-E,3R)-3-Hydroxy-12'-apo-β-carotin-12'-al* (**9**). A slurry of phosphonium salt **5** [1] (15.0 g, 29.0 mmol), 2,7-dimethylocta-2,4,6-trienedial [9] (**8**; 4.0 g, 24.2 mmol), 1,2-epoxybutane (10 ml, 115 mmol), and EtOH (30 ml) was stirred at reflux for 20 h. The mixture was evaporated and the residue (19 g) purified by flash chromatography (FC) on silica gel (2 kg) with $CHCl_3$/acetone 9:1. The crystalline residue (12.3 g) from the pure fractions was recrystallized from CH_2Cl_2 (30 ml) by slow addition of hexane (80 ml) at r.t. The product was filtered off, washed with hexane (30 ml), and dried at 60°/0.01 Torr: 5.40 g (61.1%) of **9**. M.p. 176–178°. HPLC: 98.3%. TLC ($CHCl_3$/acetone 9:1): R_f 0.35 for **9**, 0.45 for **8**, *ca.* 0.2 for **2** (isomers). UV/VIS ($CHCl_3$): 432 (1830). IR and MS in agreement with [6]. ^{1}H-NMR (400 MHz, $CDCl_3$): 9.46 (*s*, H–C(12')); 7.04 (*dd*, $J = 14.8$, 11.5, H–C(15)); 6.97 (*d*, $J = 12$, H–C(14')); 6.80 (*dd*, $J = 14.8$, 11.6, H–C(11)); 6.69 (*dd*, $J = 14.5$, 11.8, H–C(15')); 6.38 (*d*, $J = 15$, H–C(12)); 6.18 (*d*, $J \approx 12$, H–C(10)); 6.19, 6.14 (*AB*, $J = 16.5$, H–C(7), H–C(8)); 4.00 (*m*, H–C(3)); 2.40 (*dd*, $J = 16.5$, 6, H_{eq}–C(4)); 2.06 (*dd*, $J = 16.5$, 9, H_{ax}–C(4)); 2.046 (*s*, CH_3(20)); 1.993 (*s*, CH_3(19)); 1.885 (*s*, CH_3(20')); 1.78 (*ddd*, $J = 12$, 3, 1.5, H_{eq}–C(2)); 1.78 (*s*, CH_3(18)); 1.48 (*m*, H_{ax}–C(2)); 1.44 (br. *s*, OH–C(3)); 1.078 (*s*, CH_3(16), CH_3(17)); all δ in excellent agreement with [6].

4. *(7Z,3R)-3-Hydroxy-12'-apo-β-carotin-12'-al* (**10**). As described in *Exper. 3* with **4** [1] (10.34 g, 20.0 mmol), **8** (3.28 g, 20.0 mmol), 1,2-epoxybutane (7 ml, 80.5 mmol), and EtOH (20 ml). FC (silica gel (1 kg)) of the residue (16.6 g) and recrystallization of the product (7.7 g; CH_2Cl_2 (15 ml) hexane (80 ml), r.t.) as described in *Exper. 3* gave 3.80 g (51.8%) of **10**. M.p. 143–144°. HPLC: 96.2%. TLC ($CHCl_3$/acetone 9:1): R_f 0.33 for **10**, 0.45 for **8**, *ca.* 0.2 for **2** (isomers). UV/VIS ($CHCl_3$): 426 (1713). IR: 3431*s*, 2957*m*, 2923*m*, 1649*s*, 1601*s*, 1545*s*, 1188*s*, 961*s*. ^{1}H-NMR (400 MHz, $CDCl_3$): 9.456 (*s*, H–C(12')); 7.02 (*dd*, $J = 14.8$, 11.6, H–C(15)); 6.96 (*d*, $J = 12$, 14, H–C(14')); 6.71 (*dd*, $J = 14.8$, 11.8, H–C(11)); 6.68 (*dd*, $J = 14.6$, 11.6, H–C(15')); 6.34 (*d*, $J = 14.8$, H–C(12)); 6.30 (*d*, $J = 11.6$, H–C(14)); 6.23 (*d*, $J = 11.6$, H–C(10)); 6.14 (*d*, $J = ca.$ 12, H–C(8)); 5.84 (*d*, $J \approx 12.3$, H–C(7)); 4.03 (*m*, H–C(3)); 2.35 (*m*, H_{eq}–C(4)); 2.029 (*s*, CH_3(20)); *ca.* 1.97 (*m*, H_{ax}–C(4)); 1.883 (*s*, CH_3(19), CH_3(20')); 1.70 (*m*, H_{eq}–C(2)); 1.559 (*s*, CH_3(18)); 1.50 (*m*, H_{ax}–C(2)); 1.106, 1.091 (2*s*, 3 H each, CH_3(16), CH_3(17)). MS: 366 (100, M^+), 255 (10), 145 (46), 119 (70), 91 (72).

5. *(9Z,3R)-3-Hydroxy-12'-apo-β-carotin-12'-al* (**11**). As described in *Exper. 3* with **7** (7.5 g, 14.5 mmol), **8** (1.99 g, 12.1 mmol), 1,2-epoxybutane (5.1 ml, 58.2 mmol), and EtOH (70 ml). FC (silica gel (2 kg) Et_2O/hexane 2:1) of the residue (12.2 g) and recrystallization of the product (2.0 g; CH_2Cl_2 (20 ml)/hexane (60 ml), 0°) as described in

Exper. 3 gave 1.41 g (31.8%) of **11**. M.p. 151–152°. HPLC: 99.9%. TLC ($CHCl_3$/acetone 9:1): R_f 0.34 for **11**, 0.45 for **8**. UV/VIS ($CHCl_3$): 428 (1756). IR: 3460*m*, 2916*m*, 1652*s*, 1602*m*, 1550*s*, 1192*s*, 963*m*. ^{1}H-NMR (400 MHz, $CDCl_3$): 9.455 (*s*, H–C(12′)); 7.03 (*dd*, *J* = 14.8, 11.6, H–C(15)); 6.96 (*d*, *J* = 11.8, H–C(14′)); 6.88 (*dd*, *J* = 14.8, 11.6, H–C(11)); 6.68 (*dd*, *J* = 14.8, 11.6, H–C(15′)); 6.67 (*d*, *J* = 16.5, H–C(8)); 6.32 (*d*, *J* = 14.8, H–C(12)); 6.30 (*d*, *J* = 11.6, H–C(14)); 6.18 (*d*, *J* = 16.5, H–C(7)); 6.09 (*d*, *J* = 11.7, H–C(10)); 4.02 (*m*, H–C(3)); 2.43 (*m*, H_{eq}–C(4)); 2.08 (*m*, H_{ax}–C(4)); 2.036 (*s*, CH_3(20)); 1.995 (*s*, CH_3(19)); 1.887 (*s*, CH_3(20′)); 1.80 (*m*, H_{eq}–C(2)); 1.780 (*s*, CH_3(18)); 1.50 (*m*, H_{ax}–C(2)); 1.098, 1.089 (2*s*, 3 H each, CH_3(16), CH_3(17)). MS: 366 (27, M^+), 247 (6), 159 (43), 157 (52), 91 (100). Anal. calc. for $C_{25}H_{34}O_2$ (366.55): C 81.92, H 9.35; found: C 81.48, H 9.35.

6. *(7Z,9Z,3R)-3-Hydroxy-12′-apo-β-carotin-12′-al* (**12**). As described in *Exper. 3* with **6** (4.7 g, 9.08 mmol), **8** (1.49 g, 9.07 mmol), 1,2-epoxybutane (4 ml, 45.8 mmol), and EtOH (10 ml). FC (silica gel (2 kg), $CHCl_3$/acetone 9:1) of the residue (8.2 g) and recrystallization of the product (2.1 g; CH_2Cl_2 (10 ml)/hexane (50 ml), r.t., 3 times) as described in *Exper. 3* gave 0.55 g (16.5%) of **12**. M.p. 154–155°. HPLC: 98.0%. TLC ($CHCl_3$/acetone 9:1): R_f 0.34 for **12**, 0.45 for **8**, *ca.* 0.15 for **2** (isomers). UV/VIS ($CHCl_3$): 420 (1787). IR: 3518*m*, 2920*m*, 1654*s*, 1600*m*, 1549*s*, 1209*s*, 1188*s*, 960*m*. ^{1}H-NMR (400 MHz, $CDCl_3$): 9.452 (*s*, H–C(12′)); 7.02 (*dd*, *J* = 14.8, 11.8, H–C(15)); 6.95 (*d*, *J* = 11.8, H–C(14′)); 6.81 (*dd*, *J* = 14.8, 11.8, H–C(11)); 6.68 (*dd*, *J* = 14.7, 11.8, H–C(15′)); 6.63 (*d*, *J* = 12.5, H–C(8)); 6.29 (*d*, *J* = 11.8, H–C(14)); 6.28 (*d*, *J* = 14.8, H–C(12)); 6.03 (*d*, *J* = 11.7, H–C(10)); 6.00 (*d*, *J* ≈ 12, H–C(7)); 4.03 (*m*, H–C(3)); 2.36 (*m*, H_{eq}–C(4)); 2.030 (*s*, CH_3(20)); 1.97 (*m*, H_{ax}–C(4)); 1.883 (*s*, CH_3(20)); 1.83 (*s*, CH_3(19)); 1.80 (*m*, H_{eq}–C(2)); 1.152 (*s*, CH_3(18)); 1.49 (*m*, H_{ax}–C(2)); 1.41 (br. *s*, OH–C(3)); 1.114, 1.102 (2*s*, 3 H each, CH_3(16), CH_3(17)). MS: 366 (100, M^+), 173 (19), 145 (25), 113 (27), 105 (25), 91 (23).

7. *(7Z,3R,3′R)-Zeaxanthin* (**13**). A soln. of **10** (2.93 g, 8.0 mmol), **5** (4.65 g, 9.0 mmol), 1,2-epoxybutane (7 ml, 70.5 mmol), and EtOH (20 ml) was stirred at reflux for 20 h. H_2O (7 ml) was added slowly; the mixture was stirred for further 2 h without heating, whereby product crystallized. The precipitate was filtered at r.t., washed 3 times with EtOH/H_2O 4:1 (30 ml; −10°) and dried at 60°/0.01 Torr: 2.1 g (46.1%) of **13**. M.p. 164–166°. HPLC: 93.2% (and 4.4% of **2**). TLC ($CHCl_3$/acetone 9:1): R_f 0.21 for **13**, 0.33 for **10**. UV/VIS ($CHCl_3$): 440 (1487), 459 (2026), 488 (1784). IR (3430*m*, 2960*m*, 2920*s*, 1445*m*, 1363*m*, 1040*m*, 964*s*. ^{1}H-NMR: *Table 2*. MS: 568 (100, M^+), 476 (20), 157 (54), 145 (61), 119 (100), 91 (58). Anal. calc. for $C_{40}H_{56}O_2$ (568.89): C 84.45, H 9.92; found: C 84.16, H 9.95.

8. *(7Z,7′Z,3R,3′R)-Zeaxanthin* (**17**). A soln. of **8** (1.43 g, 8.7 mmol), **4** (10.34 g, 20.0 mmol), 1,2-epoxybutane (7 ml, 80.5 mmol), and EtOH (20 ml) was stirred at reflux for 20 h. The suspension was then cooled to 0°, the product was filtered off, washed with cold EtOH (30 ml; −30°), and recrystallized by gradual solvent exchange from $CHCl_3$ (200 ml) to EtOH (300 ml) by distillation at normal pressure. The precipitated product was filtered at r.t., washed with EtOH (30 ml), and dried at 60°/0.01 Torr: 2.6 g (52.6%) of **17**. M.p. 190–192°. HPLC: 96.4% of **17** (and 2.2% of **19**). TLC ($CHCl_3$/acetone 9:1): R_f 0.21 for **17**, 0.45 for **8**. UV/VIS ($CHCl_3$): 430 (1509), 455 (2142), 485 (1894). IR: 3484*m*, 2957*s*, 2920*s*, 1443*m*, 1362*m*, 1040*m*, 962*s*. ^{1}H-NMR: *Table 3*. MS: 568 (69, M^+), 157 (50), 145 (63), 119 (100), 91 (63). Anal. calc. for $C_{40}H_{56}O_2$ (568.89): C 84.45, H 9.92; found: C 84.37, H 10.03.

9. *(9Z,9′Z,3R,3′R)-Zeaxanthin* (**18**). A soln. of **8** (0.41 g, 2.50 mmol), **7** (2.97 g, 5.74 mmol), 1,2-epoxybutane (2 ml, 23.0 mmol), and EtOH (10 ml) was stirred at reflux for 20 h. The suspension was cooled to −10° and filtered. The residue was washed with cold EtOH (30 ml; −10°) and recrystallized by gradual solvent exchange from $CHCl_3$ (25 ml) to EtOH (70 ml) by distillation at normal pressure. The product was filtered off at 0°, washed with cold EtOH (15 ml; 0°), and dried at 60°/0.01 Torr: 0.62 g (43.6%) of **18**. M.p. 178–179°. HPLC: 99.7%. TLC: ($CHCl_3$/acetone 9:1): R_f 0.21 for **18**, 0.45 for **8**. UV/VIS ($CHCl_3$): 430 (1440), 452 (1965), 479 (1700). ^{1}H-NMR: *Table 3*. MS: 568 (100, M^+), 476 (18), 119 (23), 108 (18).

10. *(7Z,9Z,7′Z,3R,3′R)-Zeaxanthin* (**19**). A soln. of **10** (2.93 g, 8.0 mmol), **6** (4.65 g, 9.00 mmol), 1,2-epoxybutane (7.0 ml, 80.5 mmol), and EtOH (20 ml) was stirred at reflux for 20 h. The suspension was cooled to −10° (1 h) and filtered. The residue was washed with cold EtOH (30 ml; −10°) and dried at 60°/0.01 Torr: 1.90 g (41.8%) of **19**. HPLC: 76.8% of **19**, containing 11.7% of **22**. This material was further purified by trituration with toluene (600 ml) at 100° for 1 h; finally, it was recrystallized by gradual solvent exchange from $CHCl_3$ (100 ml) to EtOH (800 ml) by distillation at normal pressure. The product was filtered off at r.t., washed with EtOH (15 ml), and dried at 60°/0.01 Torr: 0.61 g (13.4%) of **9**. M.p. 190–192°. HPLC: 96.9%. TLC ($CHCl_3$/acetone 9:1): R_f 0.21 for **19**, 0.34 for **10**. UV/VIS ($CHCl_3$): 430 (1498), 449 (2128), 478 (1862). IR: 3396*m*, 2959*s*, 2919*s*, 1445*m*, 1364*m*, 1042*s*, 963*s*. ^{1}H-NMR: *Table 3*. MS: 568 (30, M^+), 476 (9), 157 (39), 119 (48), 91 (100). Anal. calc. for $C_{40}H_{56}O_2$ (568.89): C 84.45, H 9.92; found: C 84.24, H 10.12.

11. *(7Z,9Z,7'Z,9'Z,3R,3'R)-Zeaxanthin* (**22**). A soln. of **8** (1.64 g, 10.0 mmol) and **6** (12.72 g, 24.6 mmol) in $CHCl_3$ (100 ml) was treated with NaOMe (30% soln. in MeOH; 4.3 ml, 23.2 mmol) at 0° under inert atmosphere. After 2 h, the mixture was treated at r.t. with sat. $NaHCO_3$ soln. (150 ml). The aq. phase was extracted with $CHCl_3$ (450 ml), the org. phase dried (Na_2SO_4 (50 g)) and concentrated to 100 ml, the solvent exchanged to EtOH (200 ml) by distillation at normal pressure, and the product filtered off, dissolved in $CHCl_3$ (100 ml), and crystallized by solvent exchange to EtOH (150 ml); this procedure was repeated twice. Finally, the product was dried at 60°/0.01 Torr: 2.50 g (44.0%) of **22**. M.p. 194–195°. HPLC: 98.6%. TLC ($CHCl_3$/acetone 9:1): R_f 0.21 for **22**, 0.45 for **8**. UV/VIS ($CHCl_3$): 420 (1399), 444 (2011), 472 (1745). IR: 3299*m*, 2961*s*, 2917*s*, 1444*m*, 1369*m*, 1043*s*, 960*s*. ^{1}H-NMR: *Table 3*. MS: 568 (92, M^+), 476 (20), 157 (54), 145 (63), 119 (100), 91 (63).

REFERENCES

[1] E. Widmer, M. Soukup, R. Zell, E. Broger, H.P. Wagner, M. Imfeld, *Helv. Chim. Acta* **1990,** *73,* 861.
[2] IUPAC Carotenoid Nomenclature, *Pure Appl. Chem.* **1975,** *41,* 407.
[3] E. Broger, Eur. Pat. Appl. 1984, EP 100839.
[4] D.E. Loeber, S.W. Russel, T.P. Toube, B.C.L. Weedon, J. Diment, *J. Chem. Soc. C* **1971,** 404.
[5] A. Rüttimann, H. Mayer, *Helv. Chim. Acta* **1980,** *63,* 1456.
[6] H. Pfander, A. Lachenmeier, M. Hadorn, *Helv. Chim. Acta* **1980,** *63,* 1377.
[7] M. Soukup, E. Widmer, T. Lukac, *Helv. Chim. Acta* **1990,** *73,* 868.
[8] K. Bernhard, G. Englert, H. Mayer, R.K. Müller, A. Rüttimann, M. Vecchi, E. Widmer, R. Zell, *Helv. Chim. Acta* **1981,** *64,* 2469.
[9] O. Isler, 'Carotenoids', Birkhäuser-Verlag, Basel, 1971.
[10] J. Buddrus, *Angew. Chem.* **1968,** *80,* 535.
[11] J. Szabolcs, *Pure Appl. Chem.* **1976,** *47,* 147.
[12] P. Molnar, D. Szabolcs, *Acta Chim. Acad. Sci. Hung.* **1979,** *99,* 155.
[13] H. Mayer, *Pure Appl. Chem.* **1979,** *51,* 535.
[14] H. Pfander, *Pure Appl. Chem.* **1979,** *51,* 565.
[15] L. Zechmeister, L. Cholnoky, A. Polgar, *Chem. Ber.* **1939,** *72,* 1678.
[16] M. Baranyai, J. Szabolcs, G. Toth, *Tetrahedron* **1976,** *32,* 876.
[17] S. Hertzberg, G. Borch, S. Liaaen-Jensen, *Acta Chem. Scand., Ser. B* **1979,** *33,* 42.
[18] R. Marbet, H. Mayer, *F. Hoffmann-La Roche AG,* unpublished.
[19] H. Mayer, *Pure Appl. Chem.* **1979,** *51,* 535.
[20] K. Noack, A.J. Thomson, *Helv. Chim. Acta* **1979,** *62,* 1902.
[21] E. Märki-Fischer, U. Marti, R. Buchecker, C.H. Eugster, *Helv. Chim. Acta* **1983,** *66,* 494.
[22] G. Englert, 'NMR of Carotenoids', in 'Carotenoid Chemistry and Biochemistry', Eds. G. Britton and T.W. Goodwin, Pergamon Press, Oxford, 1982, p. 107–134.
[23] G. Englert, M. Vecchi, *Helv. Chim. Acta* **1980,** *63,* 1711.
[24] M. Vecchi, G. Englert, R. Maurer, V. Meduna, *Helv. Chim. Acta* **1981,** *64,* 2746.
[25] V. Ramamurthy, T.T. Bopp, R.S.H Liu, *Tetrahedron Lett.* **1972,** *37,* 3915.
[26] R.S.H. Liu, J.P. Zingoni, A. Kini, M. Trammell, D. Chu, A.E. Asato, T.T. Bopp, *J. Org. Chem.* **1983,** *48,* 4817.